ELSEVIER

# Phase equilibrium studying for the supercritical fluid extraction process using carbon dioxide solvent with 1.35 mole ratio of octane to ethanol mixture

K.M. Kassim [*], R. Davarnejad, A. Zainal

*School of Chemical Engineering, Engineering Campus, University Science Malaysia, 14300 Nibong Tebal, Penang, Malaysia*

## Abstract

Supercritical fluid extraction is a clean environmental chemical engineering process that has been given an interest to many researchers worldwide. The assessment of the feasibility of the extraction process utilizing a near critical solvent would be speeded up if it is possible to predict solubility data. Solubility data were measured for carbon dioxide with a mole ratio 1.35 of octane to ethanol using a phase equilibrium loading re-circulating high-pressure type apparatus at pressures up to 100 bar and at temperature 75 °C. The experimental data were then compared with calculated theoretical data which is calculated form the regular solution equations. A thermodynamic procedure is employed to each phase by applying activity coefficient expressions related to interaction parameters which are dependent on the pressure.
© 2007 Elsevier B.V. All rights reserved.

*Keywords:* Supercritical extraction; Regular solution theory; Ethanol–octane; $CO_2$ solvent; Immiscibility

## 1. Introduction

Many researchers have produced evidence suggesting that carbon dioxide is chemically reactive toward alcohols, oxygen-containing compounds in general and also produce weak complexation in condensed mixtures of these substances [1–4].

Knowledge of phase equilibria for gaseous compound plus liquid solvent systems at high temperatures and pressures are very important in many chemical processes such as gas hydrate, LNG and LPG processes [5]. Phase behavior of gaseous compounds such as ethane, propane, butane, carbon dioxide and ammonia in supercritical solvents such as hydrocarbons, alcohols and water has been studied by Haruki et al. [5].

However, percentage of octane and ethanol extraction by high pressure $CO_2$ solvent increases with a decrease of pressure in the binary systems of $CO_2$–octane and $CO_2$–ethanol respectively, but extraction percentage of ethanol is more than octane at the same conditions [3,4].

In this proposed research, the mutual feasibility of a system involving 74.1% mole ratio of ethanol to octane (as heavy

component), using supercritical and slightly sub-critical carbon dioxide solvent was studied. Theoretical data were calculated from regular solution equations and compared with the experimental data. These equations are described in detail by King et al. [6]. The estimation of the required parameters for these calculations would be difficult if the solute is a complex substance with little known information of the structural formula. An alternative procedure will be calculating the activity coefficient from the regular solution equations type which is applied to each phase.

Calculations using the proposed equation mentioned above are defined and described in this paper, together with the physical basis for applying the proposed methods under the relevant conditions. Some of the interaction parameters that are required for the calculation of activity coefficients can be calculated from the experimental data for some equilibria systems which have been mentioned in references [7,8]. The other interaction parameters have been generated by Fredenslund et al. [9]. These parameters are independent of temperature and dependent on the pressure [6,10,11]. The method of extracting the parameters has been described in references [6,11]. The obtained data, activity coefficient, Gibbs function relationships and eventually mutual solubility data are calculated

* Corresponding author. Tel.: +60 45995999x6423; fax: +60 45941013.
*E-mail address:* chqassim@eng.usm.my (K.M. Kassim).

for two equilibria phases by using regular solution equations.

## 2. Experimental

### 2.1. Materials

A solution of ethanol (99.9%, J.T. Baker) and octane (99.8%, J.T. Baker) involving 42.56% ethanol and 57.44% octane used for supercritical extraction process, using $CO_2$ (99.9%) which purchased from Mox factory. Extracted samples from the apparatus were analyzed by gas chromatography (GC).

### 2.2. Experimental procedure

The equipment used phase equilibrium re-circulation high-pressure type apparatus as shown in Fig. 1. In this apparatus the attainment of equilibrium was further assisted by magnetic stirrer which was installed in the equilibrium vessel. All units of the apparatus, i.e. the equilibrium cell (volume 500 cm$^3$), the joining tubes, vapor and liquid sample bombs (volume 50 and 40 cm$^3$), couplings and valves were made of stainless steel and designed to withstand a working pressure of 500 bar.

The part of the equipment (Fig. 1) shown within the dash line was immersed in an air bath. The temperature in the equilibrium cell was measured using a digital thermocouple, while the cell and the circuit were under vacuum, the heavy component under study (ethanol–octane as feed) was fed into the equilibrium cell. This was accomplished by first filling the reservoir ($R_1$) with about 120 cm$^3$ of this liquid. Then the liquid heavy component was allowed to go directly into the cell by turning on the valve 8 and turning off the valve 6. Having charged the cell with the heavy component, $CO_2$ at cylinder pressure was admitted to the cell. A high-pressure pump connected between the cylinder containing the contacting $CO_2$ and the cell was then switched on to pressurize the cell. At this stage in the filling pro-

cess the heaters for the cell, the air bath and the bath fan were switched on. Having brought the cell to the desired pressure, valve 6 and 3 were turned off, and the cell was carefully brought to the desired temperature. This was accomplished by fine control the heater outputs, which were gradually increased to obtain the required temperature. Equilibration and sampling would be taken when the required temperature (by controlling of the temperature indicator) and pressure (by controlling of the pressure gauge) were reached and remained constant (equilibrium condition); at the same time the pneumatic re-circulating pump and the stirrer were turned on together. Then valve 6 was opened and after a few seconds valve 3 was opened. The purpose of doing this is to avoid any droplets of solvent passing through the vapor sample bomb flow section. The pump and stirrer were left on for about 30 min, to ensure that equilibrium had been achieved, then pump and stirrer were turned off and internal valves 3, 5, 4 and 6 were kept open. The phases were then allowed to stand in contact with each other for about 30 min to allow any bubbles in the liquid to become disengaged. After the period of 30 min the vapor sample bomb and the liquid sample bomb were isolated by turning off valves 3 and 5 (for the vapor sample bomb) and valves 4 and 6 (for the liquid sample bomb). Samples of the gas and liquid phases were then extracted from vapor bomb and the liquid bomb through valves 1 and 2, respectively.

The samples taken from A and B was a vapor and liquid sample, respectively, were analyzed by GC (Perkin Elmer) which equipped with a capillary GC column (length × i.d. 30 m × 0.32 mm, $d_f$ 1.00 μm, Supelco brand).

## 3. Results and discussion

The mutual solubility of $CO_2$/ethanol–octane ternary system was studied at temperature 75 °C and at various pressures. The composition of the equilibrium phases was noted at each pressure. The mole fractions of ethanol in the liquid and vapor phases on a carbon dioxide free basis were calculated from the following
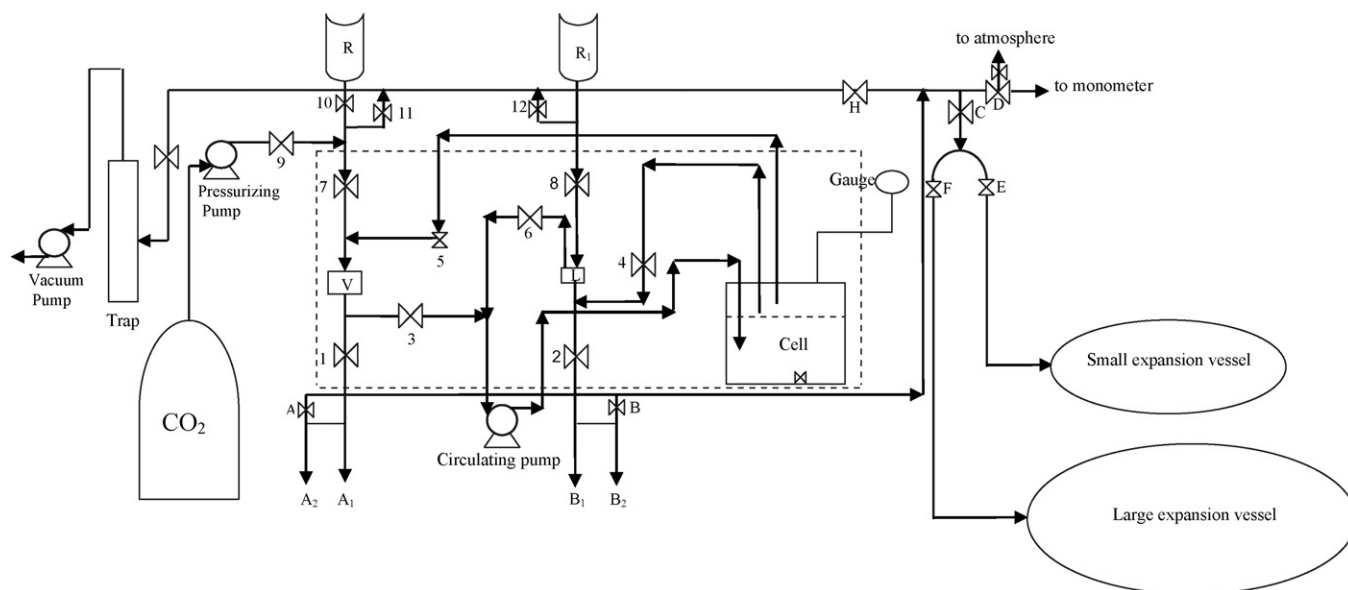


Fig. 1. Supercritical apparatus scheme.

equations:

$$X_1 = \frac{(nx_1)^L}{(nx_1)^L + (nx_2)^L} = \frac{\bar{R}}{1 + \bar{R}} \tag{1}$$

$$Y_1 = \frac{(nx_1)^G}{(nx_1)^G + (nx_2)^G} = \frac{\bar{R}_1}{1 + \bar{R}_1} \tag{2}$$

where $(nx_1)^L$ is the number of moles of ethanol in the liquid phase on a carbon dioxide free basis; $(nx_1)^G$ the number of moles of ethanol in the vapor phase on a carbon dioxide free basis; $(nx_2)^L$ the number of moles of octane in the liquid phase on a carbon dioxide free basis and $(nx_2)^G$ is the number of moles of octane in the vapor phase on a carbon dioxide free basis.

$$\bar{R} = \frac{(nx_1)^L}{(nx_2)^L}$$

$$\bar{R}_1 = \frac{(nx_1)^G}{(nx_2)^G}$$

$\bar{R}$ and $\bar{R}_1$ were read directly from the calibration chart when the ratio of the corresponding peak heights obtained from the chromatographic analyses of the liquid and vapor sample bombs were known.

The calculations for the mole fraction of carbon dioxide in the liquid phase ($X$) and in the vapor phase ($Y$) of this system were carried out using the following equations:

$$Y = \frac{(ny)^G}{(nx)^G + (ny)^G} \tag{3}$$

$$(1 - X) = \frac{(nx)^L}{(ny)^L + (nx)^L} \tag{4}$$

where $(ny)^G$ is the number of moles of carbon dioxide in the vapor sample bomb; $(nx)^G$ the number of moles of heavy component in the vapor sample bomb; $(ny)^L$ the number of moles of carbon dioxide in the liquid sample bomb and $(nx)^L$ is the number of moles of heavy component in the liquid sample bomb.

The values of $(nx)^L$ and $(nx^G)$ were calculated from the following relationship:

$$(nx)^L \text{ or } (nx)^G = \frac{\text{weight of extracted heavy components}}{x_A M_A + x_B M_B}$$

where, $x_A$ is the mole fraction of ethanol in the liquid sample bomb (or in the vapor sample bomb); $x_B$ the mole fraction of octane in the liquid sample bomb (or in the vapor sample bomb); $M_A$ the molecular weight of ethanol ($46.07 \text{ g mol}^{-1}$) and $M_B$ is the molecular weight of octane ($114.23 \text{ g mol}^{-1}$).

In the liquid bomb calculations, $x_A$ and $x_B$ were calculated from $\bar{R}$ by using the following equations:

$$x_A = \frac{\bar{R}}{1 + \bar{R}}$$

$$x_B = \frac{1}{1 + \bar{R}}$$

In order to calculate $(ny)^G$ and $(ny)^L$ it is necessary to consider deviation from the prefect gas law pressure of about 1 bar may be conveniently expressed by following equation:

$$PV = n(RT + B_v P)$$

$P$ is the pressure, $V$ the system volume, $n$ the number of moles of gas, $B_v$ is the second virial coefficient.

This equation leads directly to the expression

$$(ny)^G = V \left[ \frac{P_2}{RT + B_v P_2} - \frac{P_1}{RT + B_v P_1} \right]$$

$$= VP_2 \left[ \frac{1 - (P_1/P_2)(RT + B_v P_2/RT + B_v P_1)}{RT + B_v P_2} \right] \tag{5}$$

for the number of mole of gas in the vapor sample bomb. Where, $P_1$ and $P_2$ are expansion vessel pressure before and after expansion and $V$ is the volume of the system (35 l).

Second virial coefficient is function of system temperature, $P_1$ and $P_2$ are obtained from monometer and system temperature is obtained from temperature indicator.

The number of moles of $CO_2$ in the liquid sample bomb $(ny)^L$, was calculated by using exactly the same procedure as that given above except that total volume of the expansion system ($V$) was taken as 7 l.

Because of the proportion of heavy component extracted into the vapor phase was comparatively small, majority of it was maintained in the liquid phase without changing throughout the tests. The mole fractions of ethanol in the liquid and vapor phases were calculated on a carbon dioxide free basis at the pressures studied. The equilibrium experimental data for the system $CO_2$/ethanol–octane were listed in Table 1. This table also shows no effect of pressure on the solvent-free molar fraction of ethanol in both, the vapor and liquid phases. Two phases equilibrium data related to Table 1 based on $CO_2$ substance as function of pressure are shown in Fig. 8. It is observed that the saturation curves for the vapor and liquid phase are nearly linear. Fig. 2 shows the liquid phase composition for the system $CO_2$/ethanol–octane at 75 °C as a function of pressure. It is observed that the saturation curve for the liquid phase is nearly linear. Fig. 3 shows vapor phase composition as a function of pressure at the same temperature for the same system but the saturation curves for the vapor phase are not as linear. Fig. 4 also shows vapor and liquid composition at 75 °C and at pressure 100 bar.

The regular solution theory adopted as a model for this system is based on the activity coefficients by applying the following equations:

$$RT \ln\gamma_i = \left( \frac{d(nG_{\text{mixing}}^{\text{Excess}})}{dn_i} \right)_{T,P,n_{j\neq i}} = \left( \frac{d(nH_{\text{mixing}}^{\text{Excess}})}{dn_i} \right)_{T,P,n_{j\neq i}}$$

$$- T \left( \frac{d(nS_{\text{mixing}}^{\text{Excess}})}{dn_i} \right)_{T,P,n_{j\neq i}} \tag{6}$$

$$\ln\gamma_i = (\ln\gamma_i)^{\text{Extract}} + (\ln\gamma_i)^{\text{Solute}} \tag{7}$$

Table 1
Composition of the equilibrium vapor and liquid phase for system $CO_2$/ethanol–octane, 1.35 mole ratio of octane to ethanol mixture at 75 °C

| Pressure (bar) | Vapor phase, ethanol mole fraction on $CO_2$ free basis | Liquid phase, ethanol mole fraction on $CO_2$ free basis | Vapor phase, $CO_2$ mole fraction | Liquid phase, $CO_2$ mole fraction |
|---|---|---|---|---|
| 104.10 | 0.6480 | 0.4256 | 0.9706 | 0.9100 |
| 100.00 | 0.6540 | 0.4256 | 0.9712 | 0.8990 |
| 92.25 | 0.6630 | 0.4253 | 0.9712 | 0.8311 |
| 85.00 | 0.6722 | 0.4253 | 0.9719 | 0.7751 |
| 78.15 | 0.6820 | 0.4253 | 0.9715 | 0.7011 |
| 75.00 | 0.6850 | 0.4256 | 0.9719 | 0.6821 |
| 72.50 | 0.6882 | 0.4256 | 0.9713 | 0.6514 |
| 66.75 | 0.6960 | 0.4253 | 0.9714 | 0.5951 |
| 50.00 | 0.7200 | 0.4256 | 0.9691 | 0.4651 |
| 32.50 | 0.7480 | 0.4255 | 0.9644 | 0.2911 |

$$(\ln\gamma_i)^{\text{Extract}} = \frac{1}{RT}\left(\frac{d(nH_{\text{mixing}}^{\text{Excess}})}{dn_i}\right)_{T,P,n_{j\neq i}}$$

$$= \left(\frac{\phi^2 V_{mi}}{RT}\right)(d_i - \zeta_{ij}d_j)^2 + 2l_{ij}d_id_j\zeta_{ij} \qquad (8)$$

where

$$\zeta_{ij} = \left[\left(\frac{V_{mj}}{V_{mi}}\right)\left(\frac{q_i}{q_j}\right)\right]^{1/2} \qquad (9)$$

and

$$d_i = \left[\frac{(U_{mi}^0 - U_{mi})}{V_{mi}}\right]^{1/2} \qquad (10)$$

$d_i$ is the well known "solubility parameter" of component ($i$). $U_{mi}$ and $U_{mi}^0$ are the molar internal energy of the compressed fluid component ($i$) and the same fluid at the same temperature but a very low pressure. These parameters are calculated by
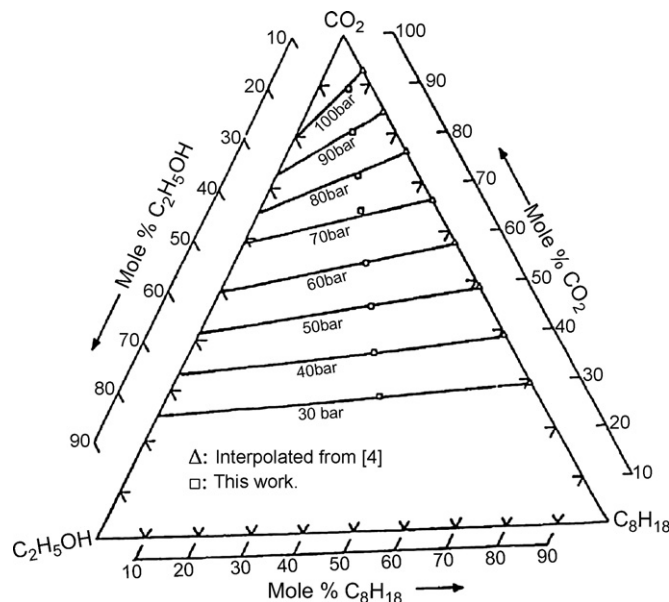


Fig. 3. Vapor composition for the system $CO_2$/ethanol–octane as function of pressure at 75 °C.
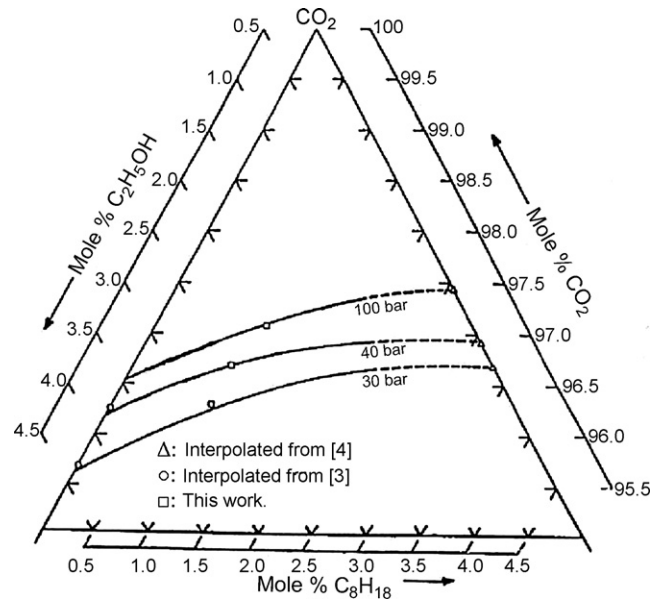


Fig. 2. Liquid composition for the system $CO_2$/ethanol–octane as a function of pressure at 75 °C.
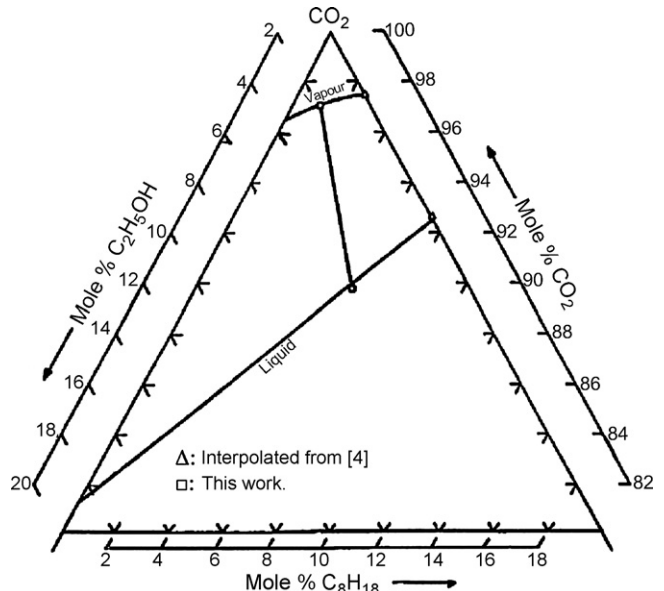


Fig. 4. Vapor and liquid composition at 75 °C and at pressure 100 bar.

the same equations but for component ($j$), as well. Eq. (8) may be compared with the expression given by the Vander Waals approach [12]

$$(\ln \gamma_i)^{\text{Extract}} = \left( \frac{\phi_j^{v^2} V_{\text{m}i}}{RT} \right) ((d_i - d_j)^2 + 2l_{ij}d_i d_j) \tag{11}$$

It only differs from Eq. (11) in the term of $\zeta$ (which is usually close to unity) and in the replacement of the area function ($\phi_j^v$) by the volume function

$$\phi_j^v = \frac{x_j V_{\text{m}j}}{x_i V_{\text{m}i} + x_j V_{\text{m}j}} \tag{12}$$

where ($V_{\text{m}i}$) is the molar volume of the pure liquid ($i$).

For a non-spherical molecule of type ($i$), quantity ($q_i$) is defined such that ($Zq_i$) is the number of interactions made by a molecular of this type with surrounding molecules. A monomer has ($Z$) interactions with nearest neighbor molecules (following X-ray diffraction information for simple fluids $Z$ is normally given a value of 10). ($q_i$) is the termed area function for the molecule. For a linear molecule [13,14]

$$q_i = r_i - \left( \frac{2(r_i - 1)}{Z} \right) \tag{13}$$

($r$) is the number of segments and it is calculated as a function of number of carbon atoms, for example ($n$) for alkanes, it can be determined by the following equation:

$$r = 0.90 + 0.283(n - 1)$$

Then arrange Eq. (8) as followed

$$\ln \gamma_i^{\text{Extract}} = \sum_{K=1}^{N} v_K^{(i)} (\ln \Gamma_K - \ln \Gamma_K^{(i)}) \tag{14}$$

$$\ln \Gamma_K = Q_K \left[ 1 - \ln \left( \sum_m^N \theta_m \Psi_{mK} \right) - \sum_{m=1}^{N} \frac{\theta_m \Psi_{Km}}{\sum_{n=1}^{N} \theta_n \Psi_{nm}} \right] \tag{15}$$

where

$$\Psi_{mK} = \text{Exp} \left( -\frac{a_{mn}}{T} \right) \tag{16}$$

$Q_k$ is the area function for group $k$ and $\theta_m$ is the area fraction of group m. $\ln \Gamma_k^{(i)}$ is defined similarly except that the group area fractions is refer to the pure liquid $i$ and not to the mixture.

$$(\ln \gamma_i)^{\text{Solute}} = \ln \left( \frac{\phi_i}{x_i} \right) + \left( \frac{Zq_i}{2} \right) \ln \left( \frac{\theta_i}{\phi_i} \right)$$

$$+ l_i - \left( \frac{\phi_i}{x_i} \right) \sum_{j=1}^{M} x_j l_j \tag{17}$$

where $M, \theta_i$ and $\phi_i$ are the number of components in the solution, the area fraction for component $i$ in the solution and the segment fraction, respectively.

$$l_i = \left( \frac{Z}{2} \right) (r_i - q_i) - (r_i - 1)$$

$$\phi_i = \frac{x_i r_i}{\sum_{i=1}^{M} x_i r_i}$$

Also there is another arrangement for Eq. (17)

$$(\ln \gamma_i)^{\text{Solute}} = \ln \left( \frac{\phi_i}{x_i} \right) - \left( \frac{Zq_i}{2} \right)$$

$$\ln \left[ 1 + \left( \frac{2\phi_j}{Zq_i} \right) \left( \left( \frac{r_i}{r_j} \right) - 1 \right) \right] \tag{18}$$

In the present work, the activity coefficient is calculated using Eqs. (7), (14) and (18).

In order to present the details calculations of the mutual solubilities for the system $CO_2$ ($i$)/heavy component (ethanol–octane mixture) ($j$) it is necessary to define that $x_i^{\text{E}}$ is the mole fraction of component $i$ based on the extract phase (carbon dioxide) and $x_i^{\text{S}}$ is the mole fraction of component $i$ based on the solute phase. Therefore $x_i^{\text{E}}$ and $x_i^{\text{S}}$ can be calculated from the activity coefficients data $\gamma_i^{\text{E}}$ and $\gamma_i^{\text{S}}$ for the phases and from the distribution factors $k_i$ and $k_j$ as

$$\gamma_i^{\text{E}} x_i^{\text{E}} = \gamma_i^{\text{S}} x_i^{\text{S}} \tag{19}$$

$$k_i = \frac{x_i^{\text{E}}}{x_i^{\text{S}}} \tag{20}$$

The procedure to calculate the mole fraction is shown as followed:

a. Guessing initial $k$-values for each component given by Eq. (20).
b. Using the guessed $k$-values to obtain the approximate mole fraction of component $i$ in each layer.

$$x_i^{\text{E}} = \frac{1 - k_j}{1 - k_j/k_i} \tag{21}$$

$$x_i^{\text{S}} = \frac{x_i^{\text{E}}}{k_i} \tag{22}$$

c. Using these first approximation values for mole fraction, the activity coefficients for component $i$ and $j$ in each phase were calculated under the given conditions using regular solution theory.
d. The activity coefficients thus obtained were used to obtain better estimates for ($k_i$) and ($k_j$) using the results

$$k_i = \frac{\gamma_i^{\text{E}}}{\gamma_i^{\text{S}}} \tag{23}$$

$$k_j = \frac{\gamma_j^{\text{E}}}{\gamma_j^{\text{S}}} \tag{24}$$

These values were then inserted into step b and the cycle was repeated until the mole fractions calculated in step b showed negligible change from one step to the next.

An alternative approach which was used in the regular solution theory calculations was to establish analytic expressions

for a function $Q$ and its derivatives with respect to mole fraction given by

$$Q_i = -[x_i \ln(x_i\gamma_i) + x_j \ln(x_j\gamma_j)] = -\frac{G_m^{mixing}}{RT} \qquad (25)$$

where ($G_m^{mixing}$) is the molar Gibbs function of mixing and from standard thermodynamic relationships.

$$\left(\frac{\partial Q_i}{\partial x_i}\right)^E = \left(\frac{\partial Q_i}{\partial x_i}\right)^S = \frac{Q_i^E - Q_i^S}{x_i^E - x_i^S} \qquad (26)$$

$$\frac{dQ_i}{dx_i} = -\ln\frac{\gamma_i x_i}{\gamma_j x_j} \qquad (27)$$

$$\frac{d^2 Q_i}{dx_i^2} = -\frac{d(\ln\gamma_i x_i/\gamma_j x_j)}{dx_i} \qquad (28)$$

where $(\partial^2 Q_i/\partial x_i^2)^E$ = gradient, $(\partial^2 Q_i/\partial x_i^2)^E$ taken at the mole fraction $(x_i^E)$ of component $(i)$ in the solvent-rich phase and $(\partial^2 Q_i/\partial x_i^2)^S$ = gradient taken at mole fraction $(x_i^S)$ of component $(i)$ in the solute-rich phase. $(\partial^2 Q_i/\partial x_i^2)$ should be negative at all points in a completely miscible system. If the system is partially miscible there will be a region which $(\partial^2 Q_i/\partial x_i^2)$ is positive. In the latter case the points on the $Q_i$ versus $x$ curve was observed corresponding to the equilibrium phase extract (E) and solute (S) which has a common tangent followed the Eq. (26).

If initial estimation of $(x_i^E)^0$ and $(x_i^S)^0$ for the mole fractions $(x_i^E)$ and $(x_i^S)$ is good and were already available, the following routine was found to be satisfactory for locating $(x_i^E)$ and $(x_i^S)$ such that Eq. (26) was accurately obeyed.

This procedure was repeated until no further adjustment was required. Eq. (26) was then satisfied and the mole fractions $(x_i^E)$ and $(x_i^S)$ specified the required calculated phase compositions.

By using the liquid–liquid equilibrium data for the system CO$_2$–hexadecane substances at various pressures and at temperature 25 °C (Fig. 5) [7,8], together with the regular solu-



Fig. 6. Regular solution theory parameter ($a_{ji}$) for CO$_2$/CH$_3$ interactions shows a function of pressure at 25 °C. These were derived from the data for the CO$_2$/n-hexadecan system as shown in Fig. 5 (i = CH$_3$ or CH$_2$ or CH and j = CO$_2$).

tion derived model to determine an effective values for the $a_{CO_2/CH_3 \text{ or } CH_2 \text{ or } CH}$ and $a_{CH_3/CO_2}$ interaction parameters as a function of pressure can be calculated (Figs. 6 and 7) [6,11]. Furthermore, the liquid–liquid equilibrium data for the system CO$_2$–heptylalcohol at exist pressure (65 bar) and at temperature 25 °C [7] were used, together with the regular solution derived model to determine the effective values for the $a_{CO_2/OH}$ and $a_{OH/CO_2}$ interaction parameters as a function of pressure. Interaction parameters were obtained $a_{CO_2/OH} = 855.51$ and $a_{OH/CO_2} = 3000$ for CO$_2$/OH and OH/CO$_2$ as an average value for the other pressures [6,11].

These data used to predict mutual miscibility of CO$_2$/ethanol–octane system at temperature 75 °C and at various pressures (Table 2). Two phases equilibrium data based on the experimental and model have been shown in Table 3, Figs. 8 and 9. The correlation related to the vapor phase between the experimental and theoretical data shows good agreement,
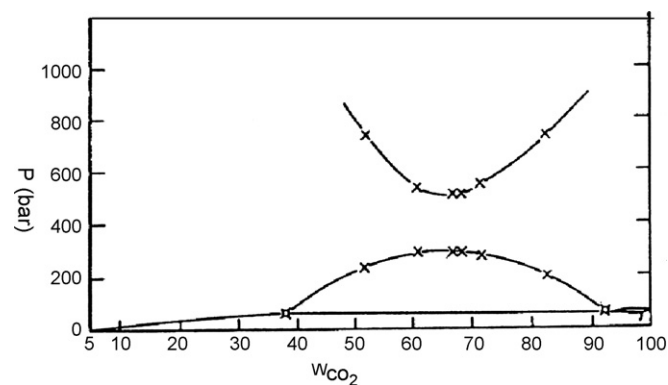


Fig. 5. Pressure–composition diagram for system carbon dioxide/n-hexadecane at 25 °C and pressure up to 1000 bar. This figure shows two regions of partial miscibility. The first, terminates at an upper critical solution pressure of about 300 bar, the second, lower critical solution pressures of about 500 bar and persists to the highest pressure studied. (×) Interpolated from [8] and (○) interpolated from [7].
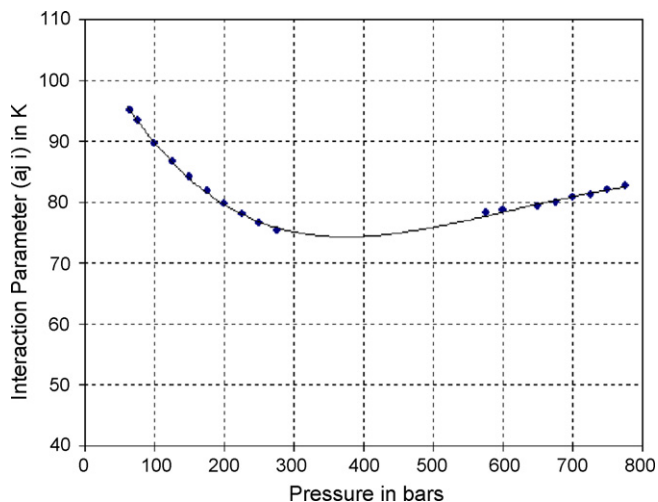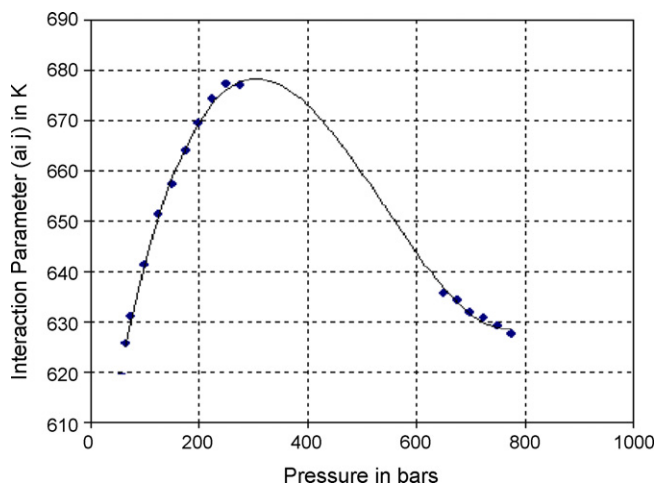


Fig. 7. Regular solution theory parameter ($a_{ij}$) for CH$_3$/CO$_2$ interactions shows as a function of pressure at 25 °C. These were derived from the data for the CO$_2$/n-hexadecan system as shown in Fig. 5 (i = CH$_3$ or CH$_2$ or CH and j = CO$_2$).

Table 2
Interaction parameters based on the experimental data extracted from references [7,8] at 25 °C

| P (bar) | $a_{CH_3/CO_2}$ | $a_{CO_2/CH_3}$ | $(x_{CO_2}^E)^{model}$ | $(x_{CO_2}^S)^{model}$ |
|---|---|---|---|---|
| 104.10 | 641.1752 | 89.5342 | 0.9516 | 0.8348 |
| 100.00 | 640.3018 | 89.5782 | 0.9519 | 0.8344 |
| 92.25 | 637.4674 | 90.8602 | 0.9755 | 0.6284 |
| 85.00 | 634.4533 | 91.9342 | 0.9574 | 0.8236 |
| 78.15 | 630.8486 | 93.2181 | 0.9598 | 0.8187 |
| 72.00 | 630.1543 | 93.5151 | 0.9603 | 0.8174 |
| 72.50 | 629.5920 | 93.6309 | 0.9605 | 0.8172 |
| 66.75 | 624.7362 | 95.3742 | 0.9633 | 0.8112 |
| 50.00 | 618.0068 | 97.9008 | 0.9667 | 0.8031 |
| 32.50 | 608.0218 | 101.119 | 0.9701 | 0.7953 |

$a_{CO_2/OH}$ calculated from $CO_2$–heptylalcohol system [7] = 855.51; $a_{OH/CO_2}$ calculated from $CO_2$–heptylalcohol system [7] = 3000.

Table 3
Comparison of the experimental and theoretical $CO_2$ mole fraction ($x_{CO_2}$) at 75 °C and at various pressures

| Pressure (bar) | $(x_{CO_2}^E)^{Exp}$ | $(x_{CO_2}^S)^{Exp}$ | $(x_{CO_2}^E)^{model}$ | $(x_{CO_2}^S)^{model}$ |
|---|---|---|---|---|
| 104.10 | 0.9706 | 0.9100 | 0.9516 | 0.8348 |
| 100.00 | 0.9712 | 0.8990 | 0.9519 | 0.8344 |
| 92.25 | 0.9712 | 0.8311 | 0.9755 | 0.6284 |
| 85.00 | 0.9719 | 0.7751 | 0.9574 | 0.8236 |
| 78.15 | 0.9715 | 0.7011 | 0.9598 | 0.8187 |
| 72.00 | 0.9719 | 0.6821 | 0.9603 | 0.8174 |
| 72.50 | 0.9713 | 0.6514 | 0.9605 | 0.8172 |
| 66.75 | 0.9714 | 0.5951 | 0.9633 | 0.8112 |
| 50.00 | 0.9691 | 0.4651 | 0.9667 | 0.8031 |
| 32.50 | 0.9644 | 0.2911 | 0.9701 | 0.7953 |

but otherwise for the correlation of the liquid phases. High error in sampling of the liquid phase may be a cause of the incoherence in liquid phases.

Figs. 10–12 and Table 4 show $CO_2$ activity coefficient ($\gamma_{CO_2}$) (calculated from Eq. (7)) against $CO_2$ mole fraction ($x_{CO_2}$) at constant temperature 75 °C and at various pressures. The interac-
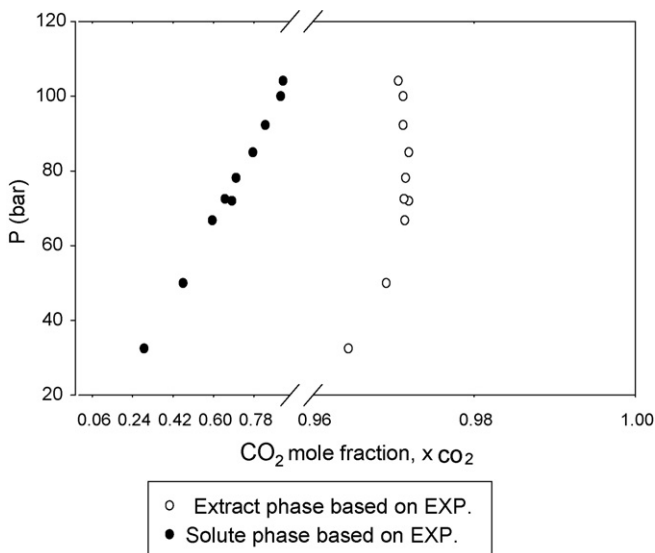


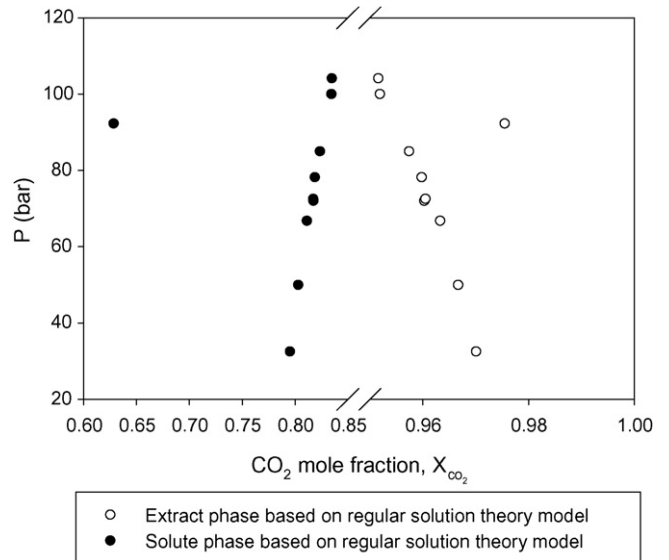Fig. 8. Two phases equilibrium data based on experiment for $CO_2$ component.



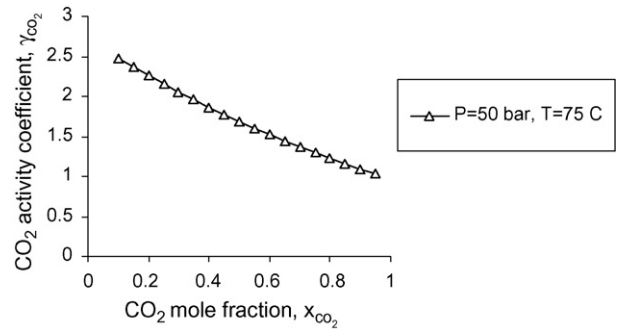Fig. 9. Two phases equilibrium data based on regular solution model for $CO_2$ component.



Fig. 10. $CO_2$ activity coefficient ($\gamma_{CO_2}$) calculated from Eq. (7) against $CO_2$ mole fraction ($x_{CO_2}$) at constant temperature 75 °C and at $P = 50$ bar.

tion parameters were obtained from Table 2 and from the tables given in reference [9]. Figs. 10–12 and Table 4 showed that carbon dioxide activity coefficients decreased with increasing carbon dioxide mole fractions.

Figs. 13–15 and Table 5 show gradient of the molar Gibbs function for $CO_2$ ($dQ_{CO_2}/dx_{CO_2}$) against $CO_2$ mole fraction at the same conditions. It is clearly shown that there are two regions exist in this experimental condition which is heterogeneous and
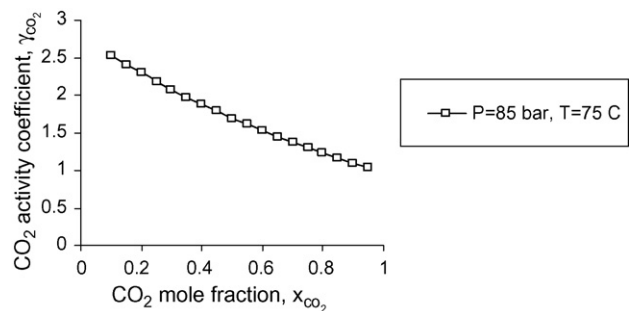


Fig. 11. $CO_2$ activity coefficient ($\gamma_{CO_2}$) calculated from Eq. (7) against $CO_2$ mole fraction ($x_{CO_2}$) at constant temperature 75 °C and at $P = 85$ bar.

Table 4
CO$_2$ activity coefficient ($\gamma_{CO_2}$) against CO$_2$ mole fraction ($x_{CO_2}$) at 75 °C and at variable pressures

| $x_{CO_2}$ | $\gamma_{CO_2}$, 104.1 bar | $\gamma_{CO_2}$, 92.25 bar | $\gamma_{CO_2}$, 78.15 bar | $\gamma_{CO_2}$, 75 bar | $\gamma_{CO_2}$, 72.5 bar | $\gamma_{CO_2}$, 66.75 bar | $\gamma_{CO_2}$, 32.5 bar |
|---|---|---|---|---|---|---|---|
| 0.1 | 2.5587 | 2.5432 | 2.5155 | 2.5128 | 2.5101 | 2.4899 | 2.4197 |
| 0.15 | 2.4316 | 2.4190 | 2.3965 | 2.3943 | 2.3920 | 2.3755 | 2.3175 |
| 0.2 | 2.3105 | 2.3005 | 2.2825 | 2.2808 | 2.2789 | 2.2656 | 2.2183 |
| 0.25 | 2.1952 | 2.1874 | 2.1732 | 2.1719 | 2.1704 | 2.1599 | 2.1221 |
| 0.3 | 2.0853 | 2.0793 | 2.0685 | 2.0676 | 2.0663 | 2.0583 | 2.0288 |
| 0.35 | 1.9805 | 1.9761 | 1.9682 | 1.9675 | 1.9666 | 1.9606 | 1.9384 |
| 0.4 | 1.8805 | 1.8775 | 1.8720 | 1.8716 | 1.8708 | 1.8667 | 1.8506 |
| 0.45 | 1.7851 | 1.7833 | 1.7798 | 1.7796 | 1.7790 | 1.7763 | 1.7655 |
| 0.5 | 1.6941 | 1.6931 | 1.6913 | 1.6912 | 1.6908 | 1.6894 | 1.6829 |
| 0.55 | 1.6070 | 1.6068 | 1.6063 | 1.6064 | 1.6061 | 1.6056 | 1.6027 |
| 0.6 | 1.5238 | 1.5242 | 1.5246 | 1.5248 | 1.5246 | 1.5249 | 1.5247 |
| 0.65 | 1.4442 | 1.4449 | 1.4461 | 1.4463 | 1.4462 | 1.4470 | 1.4489 |
| 0.7 | 1.3678 | 1.3688 | 1.3704 | 1.3706 | 1.3706 | 1.3718 | 1.3750 |
| 0.75 | 1.2945 | 1.2955 | 1.2974 | 1.2976 | 1.2977 | 1.2990 | 1.3029 |
| 0.8 | 1.2240 | 1.2250 | 1.2268 | 1.2271 | 1.2271 | 1.2284 | 1.2325 |
| 0.85 | 1.1563 | 1.1572 | 1.1587 | 1.1589 | 1.1590 | 1.1601 | 1.1637 |
| 0.9 | 1.0920 | 1.0926 | 1.0937 | 1.0938 | 1.0938 | 1.0946 | 1.0972 |
| 0.95 | 1.0340 | 1.0343 | 1.0347 | 1.0348 | 1.0348 | 1.0352 | 1.0363 |
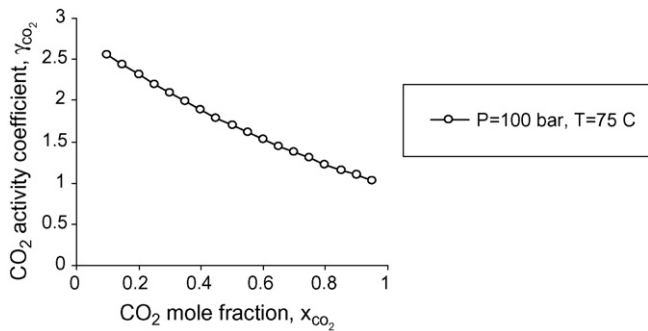


Fig. 12. CO$_2$ activity coefficient ($\gamma_{CO_2}$) calculated from Eq. (7) against CO$_2$ mole fraction ($x_{CO_2}$) at constant temperature 75 °C and at $P$ = 100 bar.



Fig. 14. Gradient of the molar Gibbs function against CO$_2$ mole fraction ($x_{CO_2}$) at constant temperature 75 °C and at $P$ = 85 bar.

homogeneous area. The heterogeneous area is for CO$_2$ mole fractions less than $x_{CO_2} = 0.35$ and the homogeneous area is for CO$_2$ mole fractions more than $x_{CO_2} = 0.35$.

In addition, Figs. 16–18 and Table 6 show second derivative of molar Gibbs function for CO$_2$ ($d^2 Q_{CO_2}/dx^2_{CO_2}$) against CO$_2$ mole fraction at the same conditions. The solubility parameter shows a negative range for a completely miscible system. If
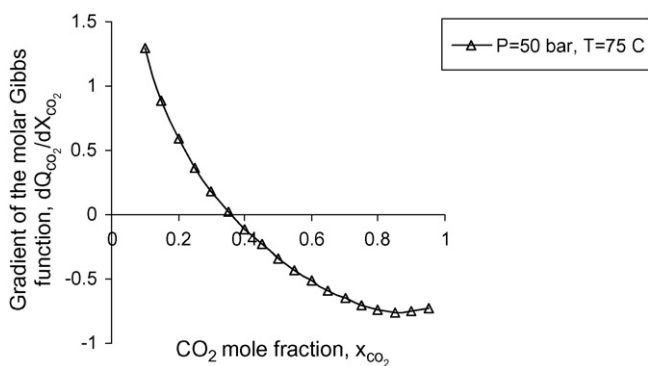
the system is partially miscible, this parameter shows a positive range. Hence, the results based on regular solution model predict that studied system is completely miscible in the whole of CO$_2$ mole fractions, except at $x_{CO_2} = 0.9$ for all of the pressures and at $x_{CO_2} = 0.95$ for pressure 32.5 bar that the system is partially miscible.



Fig. 13. Gradient of the molar Gibbs function against CO$_2$ mole fraction ($x_{CO_2}$) at constant temperature 75 °C and at $P$ = 50 bar.
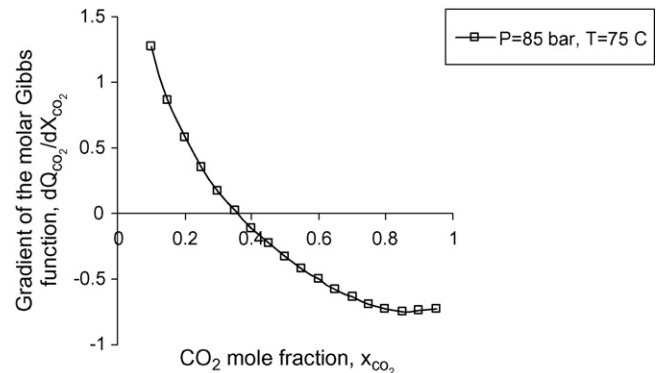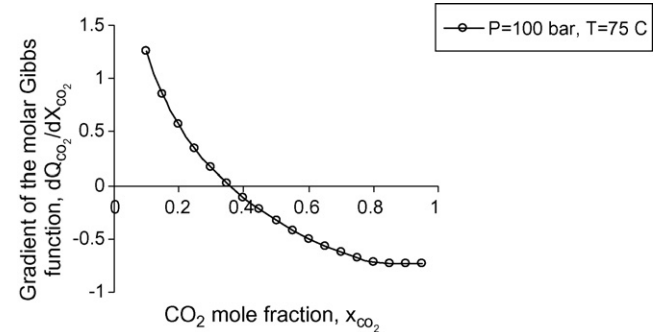


Fig. 15. Gradient of the molar Gibbs function against CO$_2$ mole fraction ($x_{CO_2}$) at constant temperature 75 °C and at $P$ = 100 bar.

Table 5
Gradient of the molar Gibbs function for $CO_2$ against $CO_2$ mole fraction ($x_{CO_2}$) at 75 °C and at variable pressures

| $x_{CO_2}$ | $dQ_{CO_2}/dx_{CO_2}$, 104.1 bar | $dQ_{CO_2}/dx_{CO_2}$, 92.25 bar | $dQ_{CO_2}/dx_{CO_2}$, 78.15 bar | $dQ_{CO_2}/dx_{CO_2}$, 75 bar | $dQ_{CO_2}/dx_{CO_2}$, 72.5 bar | $dQ_{CO_2}/dx_{CO_2}$, 66.75 bar | $dQ_{CO_2}/dx_{CO_2}$, 32.5 bar |
|---|---|---|---|---|---|---|---|
| 0.1 | 1.2632 | 1.2692 | 1.2799 | 1.281 | 1.2820 | 1.2900 | 1.3181 |
| 0.15 | 0.8588 | 0.8638 | 0.8727 | 0.8736 | 0.8745 | 0.8811 | 0.9049 |
| 0.2 | 0.5724 | 0.5763 | 0.5835 | 0.5842 | 0.5849 | 0.5903 | 0.6096 |
| 0.25 | 0.3508 | 0.3538 | 0.3591 | 0.3596 | 0.3602 | 0.3643 | 0.3791 |
| 0.3 | 0.1704 | 0.1723 | 0.1759 | 0.1762 | 0.1767 | 0.1794 | 0.1898 |
| 0.35 | 0.0186 | 0.0195 | 0.0214 | 0.0215 | 0.0218 | 0.0232 | 0.0292 |
| 0.4 | −0.1121 | −0.1121 | −0.1120 | −0.112 | −0.1119 | −0.1117 | −0.1102 |
| 0.45 | −0.2263 | −0.2272 | −0.2288 | −0.2291 | −0.2291 | −0.2302 | −0.2330 |
| 0.5 | −0.3272 | −0.3290 | −0.3323 | −0.3327 | −0.3328 | −0.3352 | −0.3423 |
| 0.55 | −0.4167 | −0.4195 | −0.4243 | −0.4249 | −0.4252 | −0.4287 | −0.4401 |
| 0.6 | −0.4963 | −0.4998 | −0.5062 | −0.5069 | −0.5073 | −0.5120 | −0.5274 |
| 0.65 | −0.5664 | −0.5708 | −0.5785 | −0.5793 | −0.5799 | −0.5855 | −0.6047 |
| 0.7 | −0.6271 | −0.6321 | −0.6409 | −0.6419 | −0.6426 | −0.6491 | −0.6715 |
| 0.75 | −0.6775 | −0.6828 | −0.6925 | −0.6935 | −0.6943 | −0.7015 | −0.7264 |
| 0.8 | −0.7152 | −0.7207 | −0.7305 | −0.7316 | −0.7325 | −0.7398 | −0.7659 |
| 0.85 | −0.7360 | −0.7410 | −0.7501 | −0.751 | −0.7520 | −0.7588 | −0.7836 |
| 0.9 | −0.7346 | −0.7379 | −0.7442 | −0.7447 | −0.7455 | −0.7503 | −0.7689 |
| 0.95 | −0.7312 | −0.7302 | −0.7288 | −0.7283 | −0.7288 | −0.7280 | −0.7287 |

Table 6
Solubility parameter ($d^2 Q_{CO_2}/dx_{CO_2}^2$) for $CO_2$ against $CO_2$ mole fraction ($x_{CO_2}$) at 75 °C and at variable pressures

| $x_{CO_2}$ | $d^2 Q_{CO_2}/dx_{CO_2}^2$, 104.1 bar | $d^2 Q_{CO_2}/dx_{CO_2}^2$, 92.25 bar | $d^2 Q_{CO_2}/dx_{CO_2}^2$, 78.15 bar | $d^2 Q_{CO_2}/dx_{CO_2}^2$, 75 bar | $d^2 Q_{CO_2}/dx_{CO_2}^2$, 72.5 bar | $d^2 Q_{CO_2}/dx_{CO_2}^2$, 66.75 bar | $d^2 Q_{CO_2}/dx_{CO_2}^2$, 32.5 bar |
|---|---|---|---|---|---|---|---|
| 0.1 | −9.9805 | −10.0009 | −10.0370 | −10.0407 | −10.0438 | −10.0699 | −10.1579 |
| 0.15 | −6.6432 | −6.6635 | −6.6995 | −6.7032 | −6.7063 | −6.7324 | −6.8208 |
| 0.2 | −4.9716 | −4.9918 | −5.0277 | −5.0314 | −5.0345 | −5.0606 | −5.1494 |
| 0.25 | −3.9656 | −3.9856 | −4.0213 | −4.025 | −4.0281 | −4.0541 | −4.1431 |
| 0.3 | −3.2914 | −3.3112 | −3.3466 | −3.3502 | −3.3533 | −3.3792 | −3.4683 |
| 0.35 | −2.8056 | −2.8252 | −2.8601 | −2.8637 | −2.8668 | −2.8925 | −2.9814 |
| 0.4 | −2.4362 | −2.4554 | −2.4898 | −2.4933 | −2.4964 | −2.5217 | −2.6101 |
| 0.45 | −2.1424 | −2.1611 | −2.1947 | −2.1981 | −2.2012 | −2.2261 | −2.3133 |
| 0.5 | −1.8988 | −1.9168 | −1.9494 | −1.9527 | −1.9557 | −1.9799 | −2.0653 |
| 0.55 | −1.6880 | −1.7051 | −1.7361 | −1.7392 | −1.7422 | −1.7653 | −1.8478 |
| 0.6 | −1.4962 | −1.5119 | −1.5407 | −1.5435 | −1.5463 | −1.5679 | −1.6459 |
| 0.65 | −1.3103 | −1.3241 | −1.3495 | −1.3519 | −1.3546 | −1.3737 | −1.4444 |
| 0.7 | −1.1154 | −1.1262 | −1.1462 | −1.148 | −1.1504 | −1.1658 | −1.2248 |
| 0.75 | −0.8906 | −0.8964 | −0.9079 | −0.9086 | −0.9106 | −0.9198 | −0.9591 |
| 0.8 | −0.6035 | −0.6009 | −0.5975 | −0.5964 | −0.5977 | −0.5960 | −0.6005 |
| 0.85 | −0.2099 | −0.1914 | −0.1600 | −0.1553 | −0.1552 | −0.1330 | −0.0706 |
| 0.9 | 0.2563 | 0.3083 | 0.3992 | 0.4114 | 0.4144 | 0.4805 | 0.6865 |
| 0.95 | −1.0030 | −0.8666 | −0.6251 | −0.5939 | −0.5835 | −0.4059 | 0.1692 |
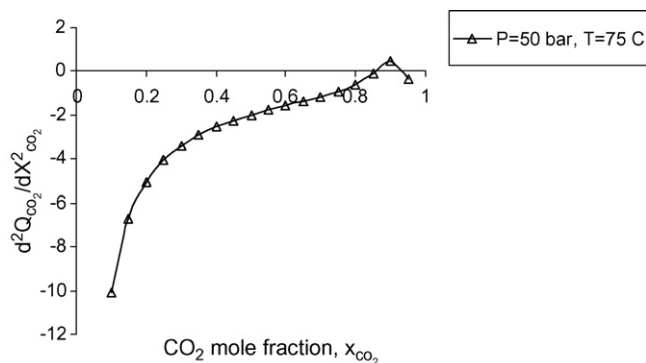
Fig. 16. Solubility parameter against $CO_2$ mole fraction ($x_{CO_2}$) at constant temperature 75 °C and at $P = 50$ bar.
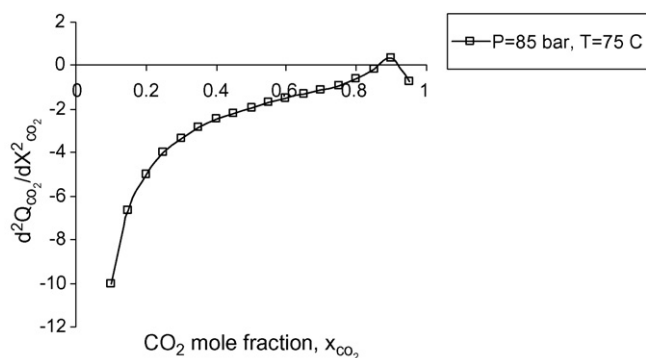


Fig. 17. Solubility parameter against $CO_2$ mole fraction ($x_{CO_2}$) at constant temperature 75 °C and at $P = 85$ bar.
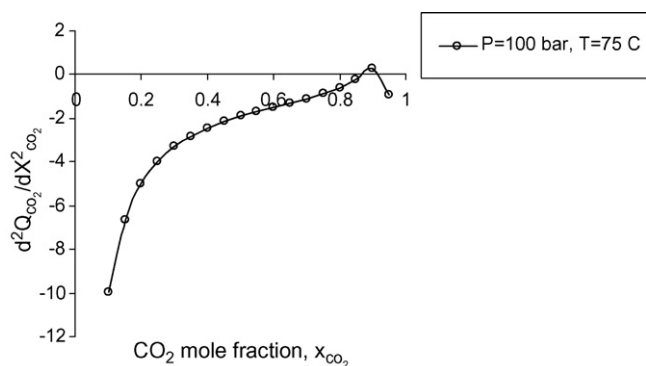


Fig. 18. Solubility parameter against $CO_2$ mole fraction ($x_{CO_2}$) at constant temperature 75 °C and at $P = 100$ bar.

## 4. Conclusion

The regular solution theory as a general model can be applied for different systems and at various conditions. The significant different between regular solution model and other models (such as equation of states) is that the later required critical constants for phase equilibria data and therefore provide vapor phase only. But for regular solution model, the data obtained are totally related to group interaction parameters and independent of tem-

perature. It is possible to predict liquid–liquid and vapor–liquid equilibria from the knowledge of structural formula of the constituent molecular species. The system miscibility also can be obtained by applying the solubility parameter which was calculated from regular solution equations. In this study the interaction between the individual groups constituting the molecules was considered and group interaction parameters were generated together with parameters that describe the size and shape of the molecules. The regular solution equations were also applied to obtain the mutual feasibility of system $CO_2$/ethanol–octane at various pressures and at temperature 75 °C. The experimental results showed that a considerable separation was not achieved in this ethanol and octane ratio.

## References

[1] W. Hempel, J. Seidel, Über verbindungen des kohlendioxyds mit wasser, aethyläther und alkoholen, Deutsche Chemische Gesellschaft Berichte 31 (1898) 2997–3001.
[2] J.H. Hildebrand, R.L. Scott, The Solubility of Nonelectrolytes, Dover Publications, New York, 1964, p. 248.
[3] S.K. Gupta, R.D. Lesslie, A.D. King Jr., Solubility of alcohols in compressed gases. A comparison of vapor-phase interactions of alcohols and homomorphic compounds with various gases. I. Ethanol in compressed helium, hydrogen, argon, methane, ethylene, ethane, carbon dioxide and nitrous oxide, J. Phys. Chem. 77 (1973) 2011–2015.
[4] D.A. Alderson, Phase equilibrium studies relevant to high pressure separation processes. PhD, Thesis, University of Birmingham, 1975.
[5] M. Haruki, Y. Shimoyama, Y. Iwai, Y. Arai, Calculation of phase equilibria for the low-boiling-point compound + solvent binary systems by group-contribution equation of state, Fluid Phase Equilib. 205 (2003) 103–114.
[6] M.B. King, K.M. Kassim, T.R. Bott, J.R. Sheldon, R.S. Mahmud, Solubility prediction using supercritical carbon dioxide solvent, Ber. Bunsenges phys. Chem. 88 (1984) 812 (Germany).
[7] A.W. Francis, Ternary systems of liquid carbon dioxide, J. Phys. Chem. (1954) 1058–1099.
[8] G. Schneider, Z. Alwani, E. Horvath, U. Frank, Phase equilibriums and critical phenomena in binary mixed systems to 1500 bars carbon dioxide with n-octane, n-undecane, n-tridecane, and n-hexadecane, Chem. Ing. Technol. 39 (11) (1967) 649–656.
[9] A. Fredenslund, J. Gmehling, P. Rasussen, Vapor–Liquid Equilibria Using Unifac., Elsevier Scientific Publication Company, Amesterdam, Oxford, New York, 1977, pp. 43–47.
[10] J.M. Smith, H.C. Van Ness, Introduction to chemical engineering thermodynamics, 4th ed., McGraw-Hill, New York, 1987, pp. 294–296.
[11] K.M. Kassim, R. Davarnejad, Mutual solubilities prediction for some oils derivatives with supercritical and slightly sub critical carbon dioxide solvent, in: International Conference on Environment, Parkroyal Hotel, Penang, Malaysia, 2006.
[12] J.H. Hildebrand, J.M. Prausnitz, R.L. Scott, Regular and Related Solutions, Van Nostrand, 1970.
[13] M.B. King, Phase equilibrium in mixtures, Pergamon Press, UK, 1969.
[14] E.A. Guggenheim, Mixtures, Oxford University Press, UK, 1952.